AEROSPACE REPORT NO.
TOR-0091(6078)-2

Relaxation Processes of Vibrationally Excited H_2O in the Mesosphere and Thermosphere

Prepared by

V. I. LANG
Space and Environment Technology Center
Technology Operations

1 September 1991

Prepared for

PHILLIPS LABORATORY
GEOPHYSICS DIRECTORATE
Hanscom AFB, MA 01731

SPACE SYSTEMS DIVISION
AIR FORCE SYSTEMS COMMAND
Los Angeles Air Force Base
P. O. Box 92960
Los Angeles, CA 90009-2960

Engineering and Technology Group

THE AEROSPACE CORPORATION
El Segundo, California

TECHNOLOGY OPERATIONS

The Aerospace Corporation functions as an "architect-engineer" for national security programs, specializing in advanced military space systems. The Corporation's Technology Operations supports the effective and timely development and operation of national security systems through scientific research and the application of advanced technology. Vital to the success of the Corporation is the technical staff's wide-ranging expertise and its ability to stay abreast of new technological developments and program support issues associated with rapidly evolving space systems. Contributing capabilities are provided by these individual Technology Centers:

Electronics Technology Center: Microelectronics, solid-state device physics, VLSI reliability, compound semiconductors, radiation hardening, data storage technologies, infrared detector devices and testing; electro-optics, quantum electronics, solid-state lasers, optical propagation and communications; cw and pulsed chemical laser development, optical resonators, beam control, atmospheric propagation, and laser effects and countermeasures; atomic frequency standards, applied laser spectroscopy, laser chemistry, laser optoelectronics, phase conjugation and coherent imaging, solar cell physics, battery electrochemistry, battery testing and evaluation.

Mechanics and Materials Technology Center: Evaluation and characterization of new materials: metals, alloys, ceramics, polymers and their composites, and new forms of carbon; development and analysis of thin films and deposition techniques; nondestructive evaluation, component failure analysis and reliability; fracture mechanics and stress corrosion; development and evaluation of hardened components; analysis and evaluation of materials at cryogenic and elevated temperatures; launch vehicle and reentry fluid mechanics, heat transfer and flight dynamics; chemical and electric propulsion; spacecraft structural mechanics, spacecraft survivability and vulnerability assessment; contamination, thermal and structural control; high temperature thermomechanics, gas kinetics and radiation; lubrication and surface phenomena.

Space and Environment Technology Center: Magnetospheric, auroral and cosmic ray physics, wave-particle interactions, magnetospheric plasma waves; atmospheric and ionospheric physics, density and composition of the upper atmosphere, remote sensing using atmospheric radiation; solar physics, infrared astronomy, infrared signature analysis; effects of solar activity, magnetic storms and nuclear explosions on the earth's atmosphere, ionosphere and magnetosphere; effects of electromagnetic and particulate radiations on space systems; space instrumentation; propellant chemistry, chemical dynamics, environmental chemistry, trace detection; atmospheric chemical reactions, atmospheric optics, light scattering, state-specific chemical reactions and radiative signatures of missile plumes, and sensor out-of-field-of-view rejection.

UNCLASSIFIED
SECURITY CLASSIFICATION OF THIS PAGE

REPORT DOCUMENTATION PAGE

1a. REPORT SECURITY CLASSIFICATION Unclassified	1b. RESTRICTIVE MARKINGS
2a. SECURITY CLASSIFICATION AUTHORITY	3. DISTRIBUTION/AVAILABILITY OF REPORT Approved for public release; distribution unlimited.
2b. DECLASSIFICATION/DOWNGRADING SCHEDULE	
4 PERFORMING ORGANIZATION REPORT NUMBER(S) TOR-0091(6078)-2	5. MONITORING ORGANIZATION REPORT NUMBER(S)
6a. NAME OF PERFORMING ORGANIZATION The Aerospace Corporation Technology Operations 6b. OFFICE SYMBOL *(If applicable)*	7a. NAME OF MONITORING ORGANIZATION Space Systems Division
6c. ADDRESS *(City, State, and ZIP Code)* El Segundo, CA 90245-4691	7b. ADDRESS *(City, State, and ZIP Code)* Los Angeles Air Force Base Los Angeles, CA 90009-2960
8a. NAME OF FUNDING/SPONSORING ORGANIZATION Phillips Laboratory 8b. OFFICE SYMBOL *(If applicable)*	9. PROCUREMENT INSTRUMENT IDENTIFICATION NUMBER F04701-88-C-0089
8c. ADDRESS *(City, State, and ZIP Code)* Geophysics Directorate Hanscom AFB, MA 01731	10. SOURCE OF FUNDING NUMBERS PROGRAM ELEMENT NO. / PROJECT NO. / TASK NO. / WORK UNIT ACCESSION NO.

11. TITLE *(Include Security Classification)*
Relaxation Processes of Vibrationally Excited H_2O in the Mesosphere and Thermosphere

12. PERSONAL AUTHOR(S)
Lang, Valerie I.

13a. TYPE OF REPORT	13b. TIME COVERED	14. DATE OF REPORT *(Year, Month, Day)*	15. PAGE COUNT
	FROM _____ TO _____	1991 September 1	51

16. SUPPLEMENTARY NOTATION

17 COSATI CODES			18. SUBJECT TERMS *(Continue on reverse if necessary and identify by block number)*
FIELD	GROUP	SUB-GROUP	H_2O (Water); Upper Atmosphere; Non-Local Thermodynamic Equilibrium; Vibrational Relaxation

19. ABSTRACT *(Continue on reverse if necessary and identify by block number)*

A review of rate constants for the relaxation of vibrationally excited H_2O is presented. This evaluation is the second in a series of reports intended to improve the state-of-knowledge regarding the chemical kinetics of the mesosphere and thermosphere. The vibrational levels discussed are limited to those presumably populated at altitudes ≥ 50 km. The collision partners of interest are the major constituents in the upper atmosphere. The recommended rate constants have been implemented in the Strategic High Altitude Atmospheric Radiance Code (SHARC 2.0), which is used to calculate background infrared radiance.

20. DISTRIBUTION/AVAILABILITY OF ABSTRACT ☐ UNCLASSIFIED/UNLIMITED ☒ SAME AS RPT. ☐ DTIC USERS	21. ABSTRACT SECURITY CLASSIFICATION Unclassified
22a NAME OF RESPONSIBLE INDIVIDUAL	22b. TELEPHONE *(Include Area Code)* / 22c. OFFICE SYMBOL

DD FORM 1473, 84 MAR — 83 APR edition may be used until exhausted. All other editions are obsolete

SECURITY CLASSIFICATION OF THIS PAGE
UNCLASSIFIED

AEROSPACE REPORT NO.
TOR-0091(6078)-2

RELAXATION PROCESSES OF VIBRATIONALLY EXCITED H_2O IN THE MESOSPHERE AND THERMOSPHERE

Prepared

V. I. Lang
Space and Environment Technology Center
Technology Operations

Approved

C. J. Rice
Target Signatures and Backgrounds Dept.

A. B. Christensen, Principal Director
Space and Environment Technology Center

CONTENTS

FIGURES

TABLES

INTRODUCTION

This review is the second in a series of reports intended to update the state-of-knowledge regarding the temperature dependence of collisional energy transfer processes by potential radiators in the mesosphere and thermosphere. At the altitudes of interest ($\geq$ 50 km), the radiating species are generally non-LTE, that is, they are not in local thermodynamic equilibrium. For this reason, the rates of spontaneous emission processes that compete with collisional relaxation processes must be included in any kinetic description of the upper atmosphere. A previous Aerospace Corporation report [TOR-0091(6078)-1, Ref. 1] described the kinetics affecting CO radiance; this report is concerned with vibrationally excited H_2O. A discussion of the non-LTE region is contained in the former.

The last major review of atmospheric kinetics that contained relaxation rates for vibrationally excited species was that of Taylor in 1974 (Ref. 2). After reviewing the literature through 1991, we concluded that there is still a need for reliable, process-specific, experimental rate data for the collisional relaxation of vibrationally excited H_2O. Recent laser-induced fluorescence experiments have improved the temperature-dependent data for the self-relaxation of H_2O and for the relaxation by O atoms. However, the temperature dependences of the relaxation pathways enabled by the dominant atmospheric species, N_2 and O_2, have not been well characterized. Ambient temperatures in the mesosphere and thermosphere typically range from 190 to 1300 K. We have compiled the available data for each relevant relaxation partner in order to obtain temperature functions. Where possible, a linear Landau-Teller form (Ref. 3) was used. Where fewer data were available, a simplified $T^{1/2}$ temperature function was estimated. The results are presented in Appendices A through C. A description of the applicability of the Landau-Teller equation is given in Ref. 1.

Since the rovibrational line strengths for H_2O have been accurately measured by high resolution spectroscopy, the vibrational band strengths are well established. The most recent version of the sum-of-lines band strengths, as compiled in the HITRAN 1991 listing (Ref. 4), have been used to calculate the spontaneous emission rates from each H_2O vibrational level. The results are described in Appendix D.

The rate constants for the energy transfer processes described here are important parameters in the calculation of radiance emitted by the upper atmosphere. The values obtained from this analysis have been incorporated into the Strategic High Altitude Radiance Code (SHARC), Version 2.0 (Ref. 5). The format for the coefficients of the rate equations listed in Table 1 has been borrowed from SHARC. The code was also used to quantify the effect of the updated rate constants on the emissions from each H_2O vibrational band. The results are summarized in Table 2 and illustrated in Figs. 2 through 4.

DATA REVIEW

Some general results and observations from our review are described in this section. Specific references, data analyses, and rate constants are presented in Appendices A through D as well as in Table 1. A vibrational energy level diagram for H_2O is given in Fig. 1, depicting the radiative processes that result in major atmospheric infrared emissions.

The V-R,T relaxation of the v_2 (010) bending level of H_2O has been studied more than any of the other collisional relaxation processes relevant to atmospheric H_2O. However, there is still an ambiguity associated with the effect of different collision partners on the v_2 relaxation rate. The data for the collision partners O_2, N_2, and Ar are combined in Fig. A1 (Appendix A) since these are not statistically different when the errors associated with the measurements are considered. Previous versions of SHARC contained the same rate for the relaxation of the $2v_2$, $3v_2$, $v_1 + v_2$, and $v_2 + v_3$ levels as for the v_2 level. This is not the best approximation that can be made for all of these higher energy levels, and, therefore, we have modified these values as described in Appendix A.

The $H_2O(010)$ level is only 39 cm^{-1} higher in energy than the $O_2(1)$ level. This allows for rapid V-V energy transfer from H_2O to O_2 in a process that is competitive with the V-R,T relaxation of $H_2O(010)$. The two processes are difficult to separate experimentally, but it can be accomplished using a carefully planned laser-induced fluorescence experiment. However, the only data currently available for the V-V relaxation of the v_2 level are acoustic data, reported with large error bars. Therefore, as shown in Fig. B1 (Appendix B), we have taken an "average" of several of these sets of data. No temperature dependence could be established over the 300 - 600 K temperature range of the data. Our rate constant, based on experimental data, is notably larger than earlier theoretical estimates made by Taylor (Ref. 2).

Previous versions of the SHARC H_2O kinetics module already contained the only experimentally measured room temperature rate constant for the V-R,T relaxation of the (001) and (100) reservoir by N_2 or O_2 (Ref. 6). Since there are no newer data available for other temperatures, we have retained this constant for those collision partners. Current model atmospheres [e.g., 1976 Standard, (Ref. 7)] generally indicate that the number density of H_2O decreases to an insignificant amount at altitudes where $O(^3P)$ could be a potential collision partner. Since laser induced fluorescence measurements near room temperature are available for the rate constant of V-T energy transfer from $H_2O(001)$ or (100) to $O(^3P)$, these data are briefly described in Appendix C for use with any non-typical model atmospheres that may have an unusually high H_2O content at high altitudes.

Table 1. Rate Coefficients for Relaxation of Vibrationally Excited H_2O
$[k_i = A_i T^{\beta i} \exp(-C_i T^{-.333} - E_i/T]$

REACTIONS	PREVIOUS COEFFICIENTS (a,b)				REVISED COEFFICIENTS(c) A_i	β_i	C_i	$*E_i$
M + H2O(010) = M + H2O(000) N2/1.0/ O2/1.0/	5.37E-10	0.0	70.0	0.0	1.13E-10	0.0	52.5	0.0
M + H2O(100) = M + H2O(020) N2/1.0/ O2/0.7/ O(^{3}P)/8.7/	4.60E-13	0.0	0.0	0.0	4.60E-13	0.0	0.0	0.0
M + H2O(001) = M + H2O(020) N2/1.0/ O2/0.7/ O(^{3}P)/8.7/	4.60E-13	0.0	0.0	0.0	4.60E-13	0.0	0.0	0.0
M + H_2O(001) = M + H_2O(100) N2/1.0/ O2/1.0/	------	----	----	----	1.20E-11	0.5	0.0	0.0
M + H2O(020) = M + H2O(010) N2/1.0/ O2/1.0/	5.37E-10	0.0	70.0	0.0	2.26E-10	0.0	52.5	0.0
M + H2O(030) = M + H2O(020) N2/1.0/ O2/1.0/	5.37E-10	0.0	70.0	0.0	3.39E-10	0.0	52.5	0.0
M + H2O(110) = M + H2O(100) N2/1.0/ O2/1.0/	5.37E-10	0.0	70.0	0.0	1.13E-10	0.0	52.5	0.0
M + H2O(011) = M + H2O(001) N2/1.0/ O2/1.0/	5.37E-10	0.0	70.0	0.0	1.13E-10	0.0	52.5	0.0
M + H2O(110) = M + H2O(030) N2/1.0/ O2/0.7/	4.60E-13	0.0	0.0	0.0	4.60E-13	0.0	0.0	0.0
M + H2O(011) = M + H2O(030) N2/1.0/ O2/0.7/	4.60E-13	0.0	0.0	0.0	4.60E-13	0.0	0.0	0.0
O2(0) + H2O(010) - O2(1) + H2O(000)	1.00E-12	0.0	0.0	0.0	2.9E-12	0.0	0.0	0.0
O2(1) + H2O(000) - O2(0) + H2O(010)	1.00E-12	0.0	0.0	55.2	2.9E-12	0.0	0.0	55.8
O2(0) + H2O(020) - O2(1) + H2O(010)	1.00E-12	0.0	0.0	0.0	5.8E-12	0.0	0.0	0.0
O2(1) + H2O(010) - O2(0) + H2O(020)	1.00E-12	0.0	0.0	0.7	5.8E-12	0.0	0.0	1.3
O2(0) + H2O(030) - O2(1) + H2O(020)	1.00E-12	0.0	0.0	0.0	8.7E-12	0.0	0.0	58.8
O2(1) + H2O(020) - O2(0) + H2O(030)	1.00E-12	0.0	0.0	-59.3	8.7E-12	0.0	0.0	0.0
O2(0) + H2O(110) - O2(1) + H2O(100)	1.00E-12	0.0	0.0	0.0	2.9E-12	0.0	0.0	0.0
O2(1) + H2O(100) - O2(0) + H2O(110)	1.00E-12	0.0	0.0	31.0	2.9E-12	0.0	0.0	31.6
O2(0) + H2O(011) - O2(1) + H2O(001)	1.00E-12	0.0	0.0	0.0	2.9E-12	0.0	0.0	0.0
O2(1) + H2O(001) - O2(0) + H2O(011)	1.00E-12	0.0	0.0	27.3	2.9E-12	0.0	0.0	27.8

Table 1. Rate Coefficients for Relaxation of Vibrationally Excited H_2O (cont.)

REACTIONS	PREVIOUS COEFFICIENTS (a,b)				REVISED COEFFICIENTS(c) A_i	β_i	C_i	$*E_i$
H2O(010) - H2O(000) + HV	18.350.0	0.0	0.0	0.0	20.33	0	0	0
H2O(020) - H2O(000) + HV	0.454	0.0	0.0	0.0	0.567	0	0	0
H2O(100) - H2O(000) + HV	3.37	0.0	0.0	0.0	5.00	0	0	0
H2O(001) - H2O(000) + HV	78.40	0.0	0.0	0.0	76.58	0	0	0
H2O(030) - H2O(000) + HV	0.003	0.0	0.0	0.0	0.0065	0	0	0
H2O(110) - H2O(000) + HV	0.349	0.0	0.0	0.0	0.7680	0	0	0
H2O(011) - H2O(000) + HV	17.22	0.0	0.0	0.0	17.23	0	0	0
H2O(020) - H2O(010) + HV	33.74	0.0	0.0	0.0	41.29	0	0	0
H2O(100) - H2O(010) + HV	0.612	0.0	0.0	0.0	1.36	0	0	0
H2O(001) - H2O(010) + HV	3.70	0.0	0.0	0.0	2.15	0	0	0
H2O(030) - H2O(010) + HV	1.11	0.0	0.0	0.0	1.21	0	0	0
H2O(110) - H2O(010) + HV	4.17	0.0	0.0	0.0	4.53	0	0	0
H2O(011) - H2O(010) + HV	65.98	0.0	0.0	0.0	71.49	0	0	0
H2O(030) - H2O(020) + HV	36.87	0.0	0.0	0.0	40.06	0	0	0
H2O(000) + HV - H2O(010)	0.0	0.0	0.0	0.0	--------	--	--	--
H2O(000) + HV - H2O(020)	0.0	0.0	0.0	0.0	--------	--	--	--
H2O(000) + HV - H2O(100)	0.0	0.0	0.0	0.0	--------	--	--	--
H2O(000) + HV - H2O(001)	0.0	0.0	0.0	0.0	--------	--	--	--
H2O(000) + HV - H2O(030)	0.0	0.0	0.0	0.0	--------	--	--	--
H2O(000) + HV - H2O(110)	0.0	0.0	0.0	0.0	--------	--	--	--
H2O(000) + HV - H2O(011)	0.0	0.0	0.0	0.0	--------	--	--	--
H2O(010) + HV - H2O(020)	0.0	0.0	0.0	0.0	--------	--	--	--
H2O(010) + HV - H2O(100)	0.0	0.0	0.0	0.0	--------	--	--	--
H2O(010) + HV - H2O(001)	0.0	0.0	0.0	0.0	--------	--	--	--
H2O(010) + HV - H2O(030)	0.0	0.0	0.0	0.0	--------	--	--	--
H2O(010) + HV - H2O(110)	0.0	0.0	0.0	0.0	--------	--	--	--
H2O(010) + HV - H2O(011)	0.0	0.0	0.0	0.0	--------	--	--	--
H2O(020) + HV - H2O(030)	0.0	0.0	0.0	0.0	--------	--	--	--

a) R. L. Taylor, Can. J. Chem., **52**, 1381 (1974) and/or SHARC versions < 2.0.
b) This review.
* The E_i terms (i.e., the energy differences between levels) are not listed here for the V-T processes because these are obtained from the H_2OSTAT.DAT file in SHARC 2.0.

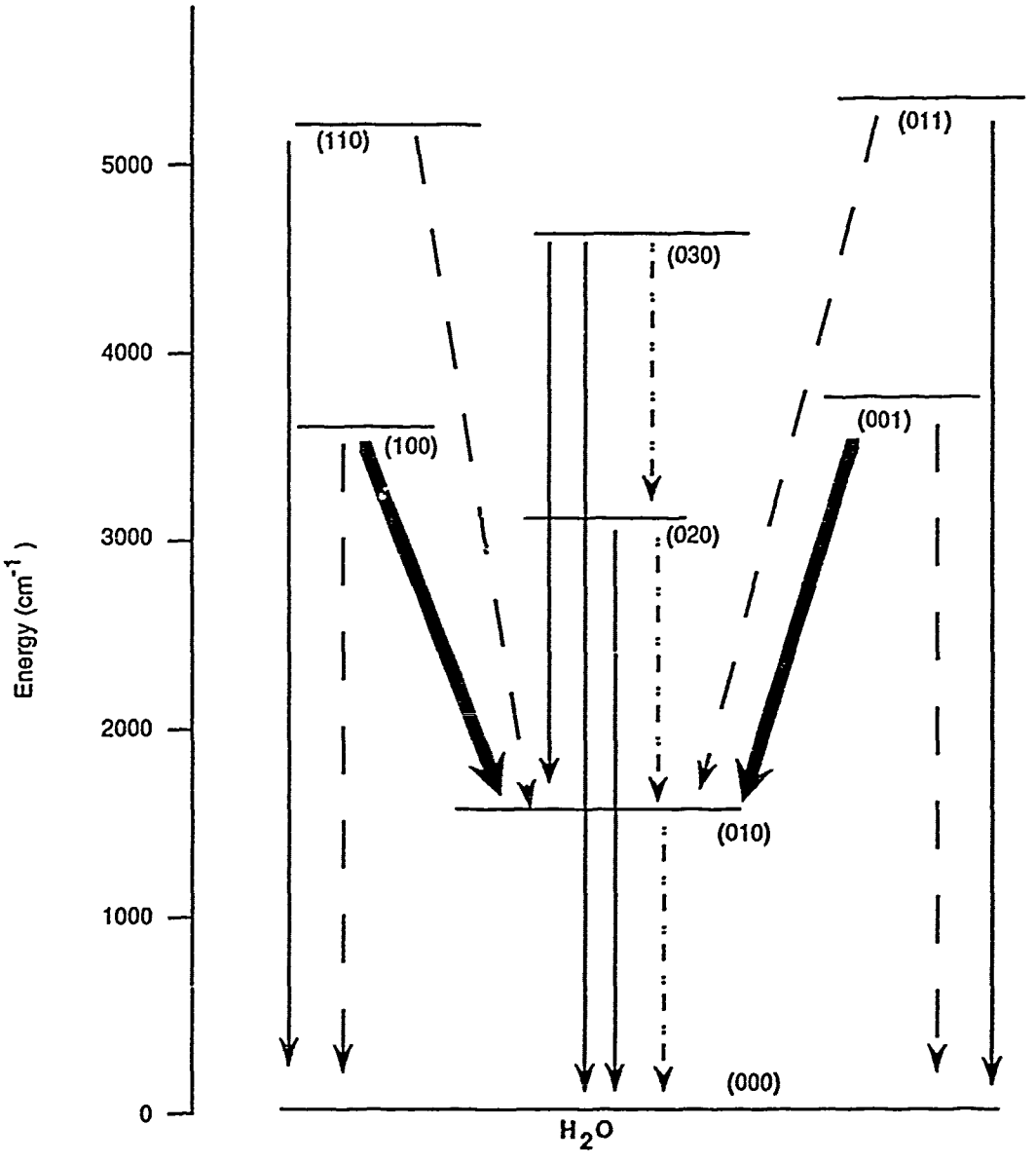

Figure 1. Vibrational bands contributing to H_2O infrared emissions in the upper atmosphere. Prominent atmospheric features occur near 6.4 mm - - - - - - , 4.7 μm ▬▬ and 2.7 μm — — — .

Einstein A coefficients for all the relevant radiative relaxation processes of vibrationally excited H_2O have been calculated using the 1991 HITRAN sum-of-lines band strengths, S_{ul}. Changes to certain H_2O rovibrational lines have been made to the HITRAN listing since the 1986 version (Ref. 8). Some of the emission rates we calculated were approximately twice as high as those previously used in SHARC. Although the line list for H_2O has been improved since 1986, the changes are not large enough to cause such significant differences in the band strengths. Rates calculated from the first coefficients of the transition dipole moments reported in the literature rather than from the band strengths may have been the source of the discrepancy. Dipole moment calculations are not straightforward for many H_2O transitions since Fermi and Coriolis interactions occur between closely spaced vibrational levels. In most cases, the full functional form of the transition dipole necessary for calculating a band strength is not explicitly given by the authors who reported H_2O line strengths. We have attempted to standardize the emission rates using the S_{ul} values so that discrepancies in the application of the theoretical parameters for the vibrational and rovibrational interactions can be avoided.

SHARC RADIANCE OUTPUT

The updates described above have been incorporated into a new input file for the ambient H_2O kinetics module in SHARC. These rates are given in Table 1 in the format currently used in SHARC (Version 2.0, Aerospace Corporation preliminary copy). A test calculation using a SHARC model atmosphere profile was performed. A subarctic daytime model atmosphere was used since the lower altitude concentrations of H_2O are larger than those in the Standard 1976 models. The results of the test are presented in Table 2 and Figs. 2 through 4. A limb view at 64 km tangent height was used with an arbitrary latitude and longitude of (0,0) chosen for illustrative purposes only. Ideally a region-specific equatorial model with large column densities of H_2O would have been preferred.

The radiances calculated by SHARC using the new kinetics scheme are generally smaller than or equal to those calculated with the old rates. The band radiances for each H_2O vibrational transition and the ratios (old:new) are listed in Table 2. The decreased emissions are a result of increasing the collisional relaxation rates of the upper vibrational levels, or effectively quenching the excited molecules before they can radiate. This effect apparently dominates over the increases made to some of the spontaneous emission rates. Transitions originating in the $3\nu_2$ level (centered at 4667 cm^{-1}, 3072 cm^{-1}, and 1515 cm^{-1}) are a factor of 12.6 times weaker after changing the kinetics. Similarly, transitions originating in the $2\nu_2$ level are 5.2 times weaker. The overall effect on the radiance in particular cm^{-1} regions is illustrated in Figs. 2 through 4. Our calculations indicate that the (020) - (000) band centered at 3150 cm^{-1} will be narrower due to less intense radiance on the high frequency side than previously predicted. This effect is evident in Fig. 4. Such changes to the more intense H_2O infrared bands have important consequences for atmospheric sensor development.

Table 2. Band Radiance Comparison

Transition	Frequency	Band Radiance ($W/sr \cdot cm^2$) Old Kinetics	New Kinetics	Radiance Ratio Old:New
(010)-(000)	1594.750	0.37277e-6	0.35466e-6	1.05
(020)-(000)	3151.630	0.11184e-8	0.21412e-9	5.22
(100)-(000)	3657.053	0.87024e-9	0.47780e-9	1.82
(001)-(000)	3755.930	0.35921e-7	0.36124e-7	0.994
(030)-(000)	4666.793	0.11070e-11	0.87792e-13	12.6
(110)-(000)	5234.977	0.63862e-11	0.24911e-11	2.56
(011)-(000)	5331.269	0.20763e-8	0.12812e-8	1.62
(020)-(010)	1556.880	0.39202e-7	0.75069e-8	5.22
(100)-(010)	2062.303	0.13254e-9	0.73330e-10	1.81
(001)-(010)	2161.180	0.16949e-8	0.16950e-8	1.00
(030)-(010)	3072.043	0.17710e-9	0.14089e-10	12.6
(110)-(010)	3640.227	0.39018e-10	0.15291e-10	2.55
(011)-(010)	3736.519	0.82490e-8	0.50967e-8	1.62
(030)-(020)	1515.163	0.32288e-8	0.25724e-9	12.6
Pure Rotational Lines		0.99151e-10	0.99151e-10	1.0
Total Overlap Corrected Bandpass Radiance		0.46488e-6	0.40686e-6	1.14

Model Atmosphere: DAYSUBAR.DAT
Lat. 0°, Long. 0°
Solar Zenith Angle 0°

Limb View, 64 km Tangent

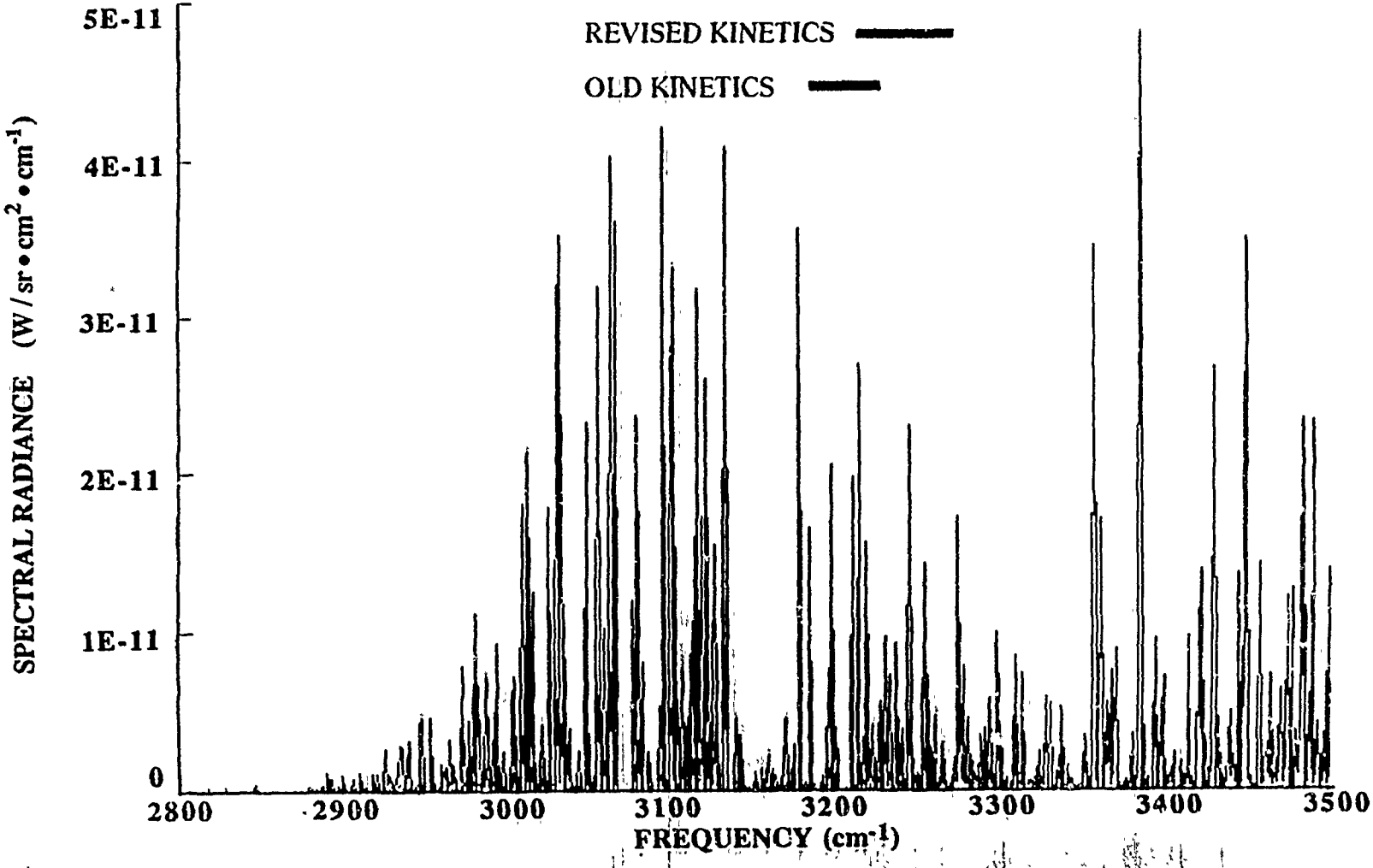

Figure 2. SHARC 2.0 limb calculation of H_2O infrared radiance using old kinetics (Ref. 2) and revised constants (this review). Main feature in this region is the (020) - (000) rovibrational band.

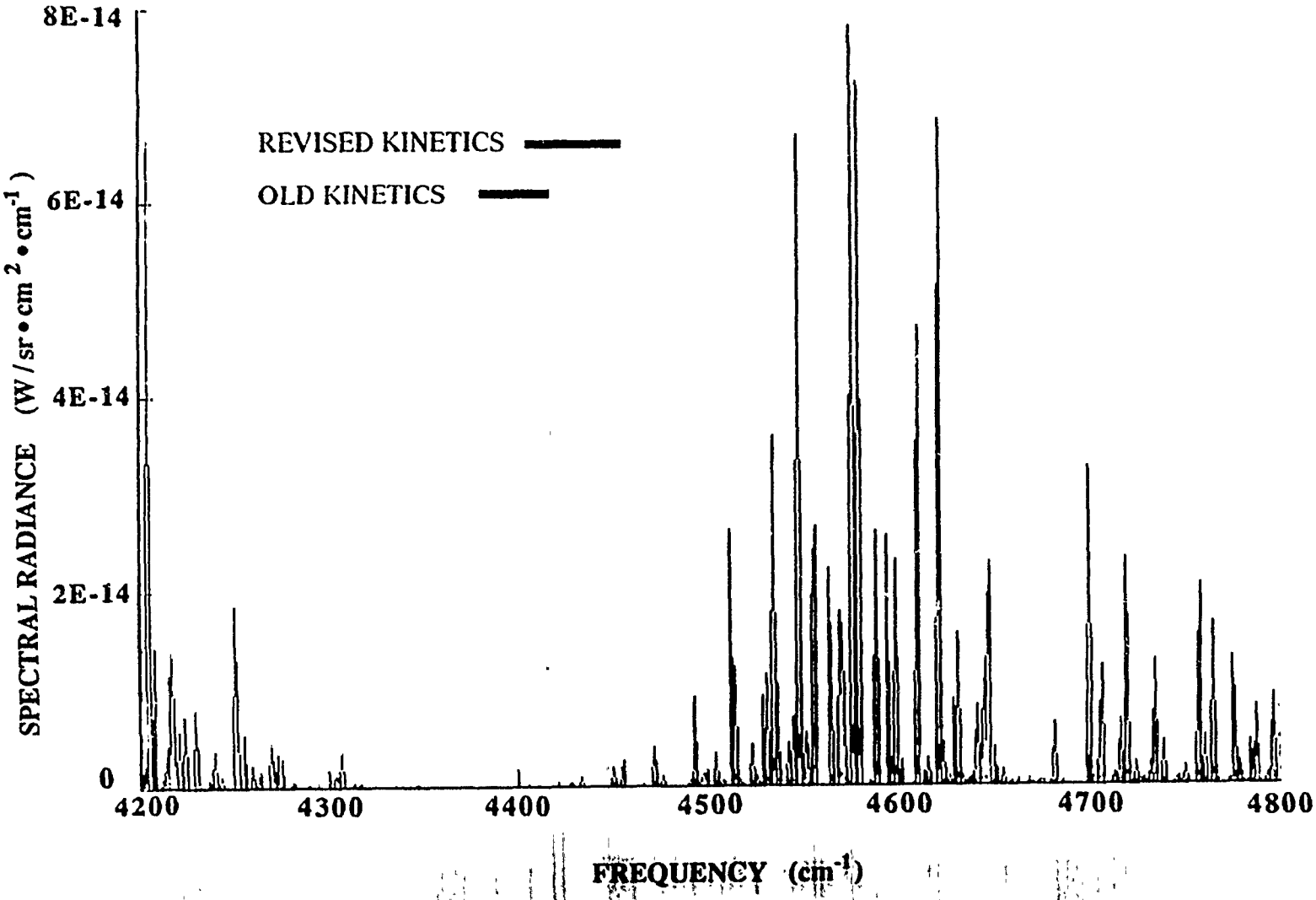

Figure 3. SHARC 2.0 limb calculation of H_2O infrared radiance. Main feature in this region is the (030) - (000) rovibrational band.

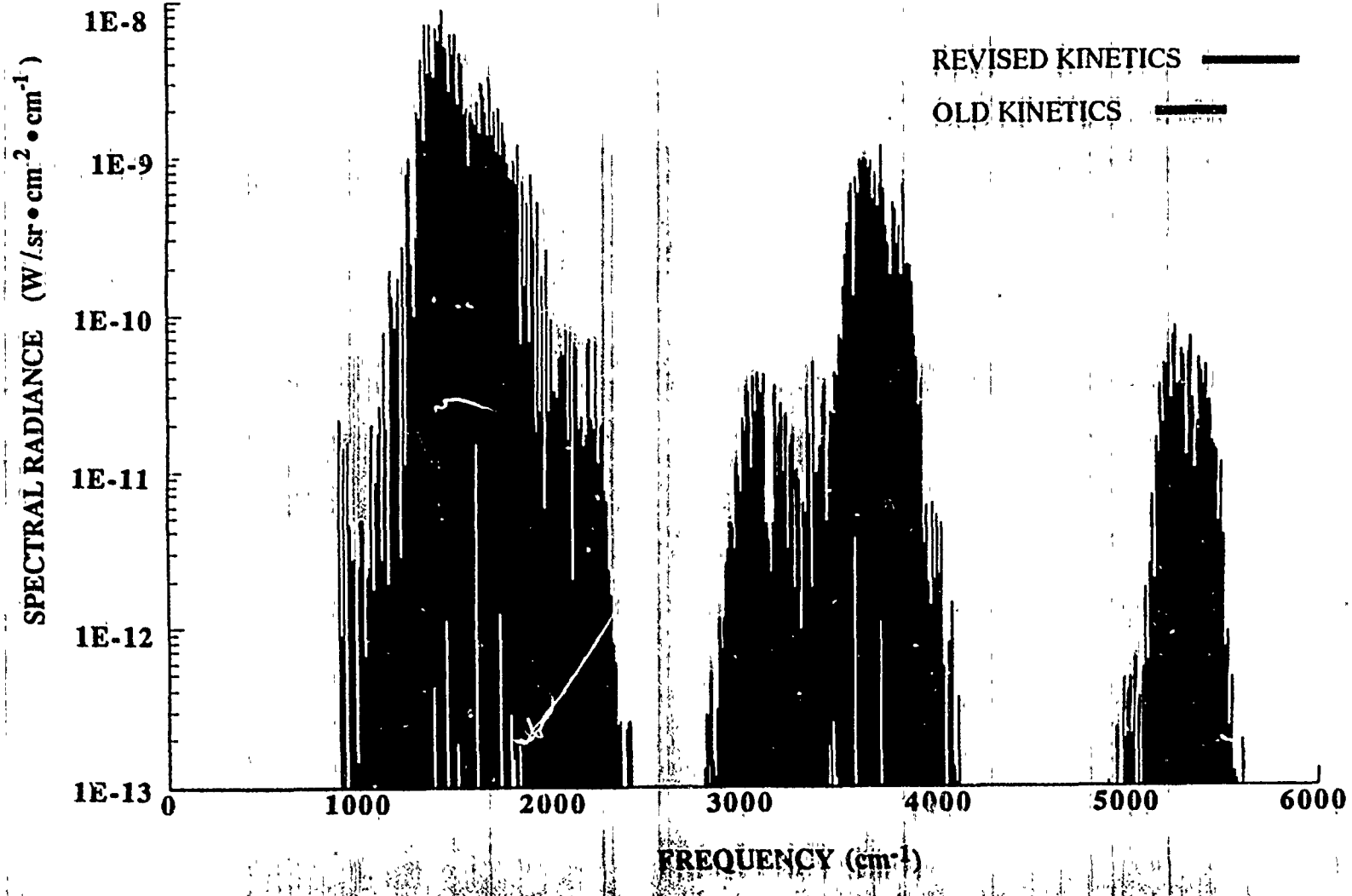

Figure 4. SHARC 2.0 limb calculation of H_2O infrared radiance. Effect of revising the relaxation rate constants is illustrated.

SUMMARY

While there is still room for improvement in experimental measurements of the $H_2O(010)$ vibrational relaxation processes, some progress has been made since 1974 when several of the rates reported by Taylor were based on theoretical inferences.

Essentially all of the individual collisional relaxation processes need further experimental investigation as a function of temperature. Laser-induced fluorescence techniques would be particularly useful in verifying previous acoustic measurements as well as accumulating data in the temperature region below the shock-tube limit and above room temperature. The V-V and V-T contributions to the overall relaxation of the ν_2 bending level by O_2 still need to be quantified.

Since the vibrational line strengths for the H_2O emission bands used in radiance codes such as SHARC have been accurately measured by high-resolution infrared spectroscopy, the spontaneous emission coefficients are well established.

REFERENCES

1. V. I. Lang, Aerospace Report Number TOR-0091(6078)-1, The Aerospace Corporation, Los Angeles, CA (1991).
2. R. L. Taylor, Can. J. Chem., **52**, 1381 (1974).
3. L. Landau and E. Teller, Phys. Zeit. Sowjetunion, **10**, 34 (1936).
4. L. S. Rothman et al., *HITRAN 1991 Line List*, Phillips Laboratory/GPS (1991) and ibid., J. Quant. Spectrosc. Rad. Transfer, to be published.
5. R. D. Sharma et al., *Description of SHARC -2 The Strategic High-Altitude Atmospheric Radiance Code*, PL-TR-91-2071, Phillips Laboratory,Hanscom AFB, MA (1991).
6. J. Finzi et al., J. Chem. Phys., **67**, 4053 (1977).
7. *U. S. Standard Atmosphere, 1976*, NOAA, NASA and U.S. Air Force, Washington, D.C., pp. 212-227 (1976).
8. L. S. Rothman et al., Appl. Opt., **26**, 4058 (1987).

APPENDIX A

V-R,T RELAXATION OF H_2O ν_2 BEND AND ν_2 COMBINATION LEVELS

a) Relaxation of ν_2 by O_2 and N_2

The two predominant [illegible] the mesosphere that can act as collision partners for vibrationally excited H_2O [illegible]. The non-radiative relaxation from the ν_2 level can be expressed as

$$M + H_2O\,(010) \xrightarrow{k_1} M + H_2O\,(000) \qquad M = N_2, O_2 \qquad (A1)$$

The H_2O kinetics module in earlier versions of SHARC contained the following temperature dependence for the V-T (or V- R,T) relaxation of the ν_2 level of H_2O:

$$k_1^{old}{}_{forward} = 5.37e\text{-}10 \exp(-69.918/T^{.335}) \qquad 200 - 400\ K \qquad (A2)$$

This rate equation is from the 1974 review article by Taylor (Ref. A1) and has a quoted uncertainty of an order of magnitude. The original research on which this Arrhenius equation is based was that of Monk (Ref. A2), who only measured rates at 295 K, using a sound absorption technique. It appears that Taylor derived an average rate constant for the relaxation of $H_2O(010)$ by N_2 + O_2 from two room temperature values (which differ by a factor of 23) and then applied a theoretical temperature dependence. That O_2 and N_2 are equally efficient partners is a reasonable assumption for the V-R,T relaxation of $H_2O(010)$. However, Monk's data are too widespread to support this assumption (see Fig. A1). Another problem lies in the relative magnitudes of Monk's data. It is inherently difficult to separate the near-resonant V-V energy transfer from $H_2O(010)$ to $O_2(100)$ from the V-T relaxation of $H_2O(010)$ by O_2. However, if the V-T contribution to the overall relaxation process is approximately the same as the V-T rate with N_2, this fraction could be subtracted from the overall O_2 rate. The major inconsistency in Monk's data is the fact that the V-T rate with O_2 is reported to be 23 times slower than that with N_2. We would expect the former to be larger by a small amount.

In all of the low temperature studies (295 - 600 K) reported in the literature (Refs. A2, A3 and A4), the acoustic techniques used to derive relaxation rate constants for Reaction A1 depend on the validity of approximations made for several concurrent energy transfer processes in a mixture of gases. The experiments were generally designed to study the dependence of Napier frequencies (frequency of maximum sound absorption per meter) as a function of O_2 and H_2O concentrations in gaseous mixtures such as air. While only a few rates were actually

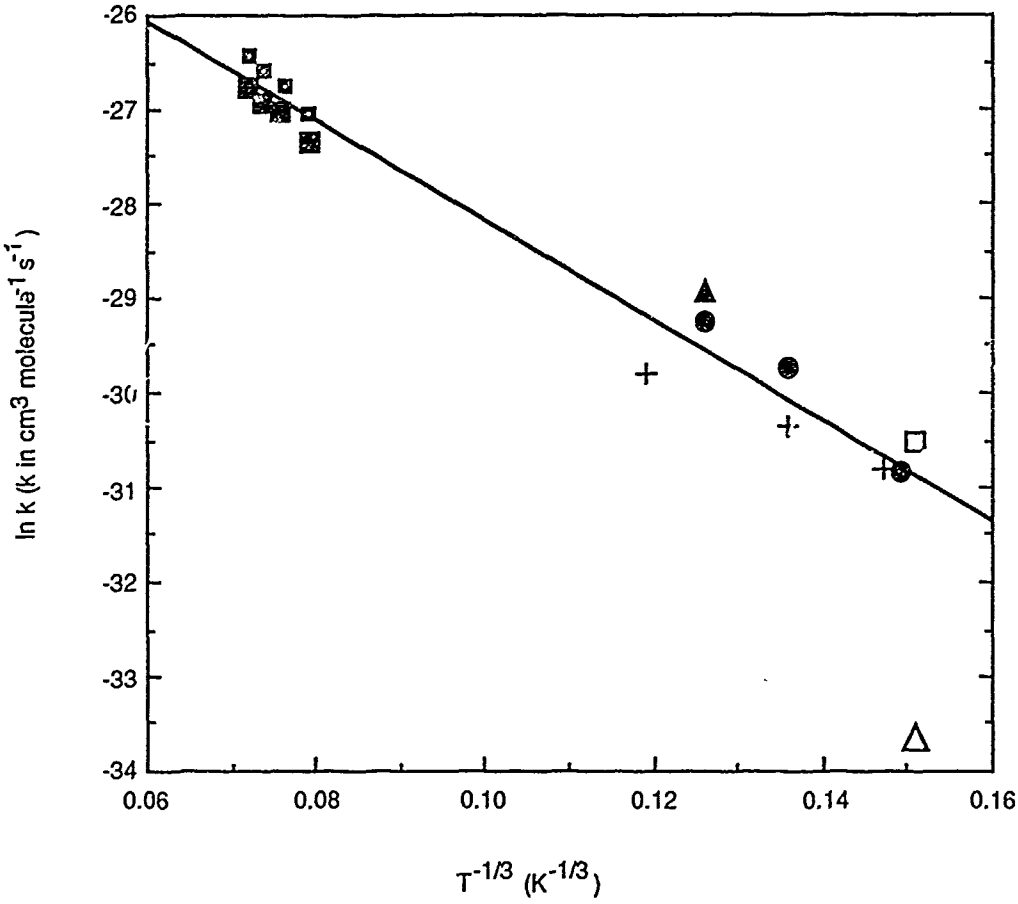

Figure A1. √-R,T relaxation of $H_2O(010)$. Data used in present fit: Kung and Center (Ref. A6), N_2 ■, Ar ■; Bass et. al. (Ref. A3), O_2 ●; Keeton and Bass (Ref. A4), N_2 or Ar ▲; Bass and Shields (Ref. A5),O_2+. Data used bv Taylor (Ref. A1) and not included in present fit: Monk (Ref. A2), O_2 Δ , N_2 □.

measured, five to seven reversible energy transfer processes were needed to stoichiometrically balance the Napier problem and to fit the experimental frequencies to a concentration curve. Examination of the procedures used by several investigators reveals that those employed by Bass, Keeton, and Williams (Ref. A3) are more self-consistent than those of earlier investigators (Monk, Ref. A2). However, the conclusions drawn by Bass et al. are questionable because they erroneously plotted data from other sources (e.g., Kung and Center, Ref. A6) as well as from their own tables.

Without going into the details of the various approximations made by different investigators, we report here the most consistent of the results from the acoustic experiments (Ref. A3, A4 and A5) for 400, 500 and 600 K. However, the individual data points from these references are not necessarily experimentally unique. The author Bass was involved in each of these studies and has incorporated the actual measurements into an iterative fitting procedure to compute the temperature dependence given in Ref. A3. We have combined the accumulated acoustic data with high temperature shock tube data for the collisional relaxation rates of H_2O (010). The latter data were taken from the original paper by Kung and Center (Ref. A6). A statistical energy distribution using the heat capacity, C_v, and the vibrational temperature, θ_T, was applied to the experimentally measured rates to correct for bulk heating inherent in the shock tube method. The authors estimate that their rate constants are accurate to within a factor of 2.

In summary, it is recommended that the functional form of the temperature dependence for the H_2O (010) V-T relaxation be updated to reflect the experimental shock tube data and the consensus of the acoustic data. In our analysis, we assumed that the V-T transfer efficiencies of N_2 and O_2 are approximately equal. We used the data for the relaxation of H_2O by Ar as well as by O_2 and N_2 since the molecular mass of O_2 lies between that of Ar and N_2. The temperature dependence obtained from fitting the combined data to a Landau-Teller function (see Fig. A1) is

$$k_1^{new} = 1.13 \times 10^{-10} \exp(-52.5/T^{.333}) \qquad 295 - 2000 \text{ K} \qquad \text{(A3)}$$

The $T^{-.333}$ coefficient was obtained from the slope of Fig. A1 while the pre-exponential factor is equal to the exponential of the ordinate intercept. At 300 K, the rate constant from Taylor's function is 1.5×10^{-14} cm^3 molecule^{-1} s^{-1} compared with our new value of 4.4×10^{-14} cm^3 molecule^{-1} s^{-1}. However, this factor-of-3 difference decreases as the temperature increases from room temperature up to ~1500 K.

The rate for the corresponding reverse process (i.e., collisional excitation of H_2O in the v_2 mode) includes the energy difference [$E_1 = \Delta E$ (cm^{-1} x 1.44 K/cm^{-1})] between ground state H_2O and H_2O (010). That is,

$$k_1^{new}{}_{reverse} = 1.13 \times 10^{-10} \exp(-52.5/T^{.333} - 2296.4/T) \quad \text{(A4)}$$

where the band ν_2 band center frequency is 1594.74 cm^{-1}. Since the SHARC 2.0 code accesses the H_2O States file for the E_l variable for the V-R,T relaxation processes, these are not listed in Table 1. The energies of the vibrational bands can also be found in the 1991 HITRAN (Ref. A7) line list.

Since the low temperature rate constants for the relaxation of H_2O by N_2 and O_2 contain so much uncertainty (~ order of magnitude) it would be worthwhile to measure the rates over the 180 - 1000 K temperature range using laser-induced fluorescence (LIF). The bulk methods previously employed for the study of ν_2 lack the capability of selective excitation of a particular level. LIF has been used successfully to study other collision partners and other vibrationally excited levels of H_2O (e.g., Refs. A8, A9).

b) V-R,T Relaxation of the $2\nu_2$ and $3\nu_2$ Levels

In previous versions of SHARC, k_1 for the V-R,T relaxation of the H_2O (010) level by N_2 and O_2 was also used for the hot emission bands, $3\nu_2 - 2\nu_2$ and $2\nu_2 - \nu_2$. Using the harmonic oscillator approximation, the rates for these V-T relaxation mechanisms of H_2O would be 3 and 2 times greater, respectively, than that for the $\nu_2 - 0$ fundamental process. The revised rate expressions for collisional relaxation with equal efficiency by M = O_2 or N_2 are

$$M + H_2O(020) = M + H_2O(010);$$

$$k_2^{new}{}_{forward} = 2.26 \times 10^{-10} \exp(-52.5/T^{.333}) \text{ and} \quad \text{(A5)}$$

$$k_2^{new}{}_{reverse} = 2.26 \times 10^{-10} \exp(-52.5/T^{.333} - 2241.9/T) \quad \text{(A6)}$$

and

$$M + H_2O(030) = M + H_2O(020);$$

$$k_3^{new}{}_{forward} = 3.39 \times 10^{-10} \exp(-52.5/T^{.333}) \text{ and} \quad \text{(A7)}$$

$$k_3^{new}{}_{reverse} = 3.39 \times 10^{-10} \exp(-52.5/T^{.333} - 2181.8/T) \quad \text{(A8)}$$

The band center frequencies of 1594.74 cm^{-1}, 3151.63 cm^{-1} and 4666.8 cm^{-1} for the ν_2, $2\nu_2$, and $3\nu_2$ levels, respectively, were used to obtain the energy difference terms for the reverse processes.

Since the rate coefficients for the overtone transitions from $3\nu_2$ and $2\nu_2$ to the ground state are assumed to be much smaller than those for transfer of a single quantum of vibrational energy, they are not included in our overall kinetics scheme.

Experimental evidence for the validity of using the harmonic oscillator approximation for the case of H_2O vibrational relaxation has been found in laser-induced fluorescence studies (Ref. A8 and A10). This is worth mentioning here because it might be expected that strong dipole interactions or hydrogen bonding by H_2O would result in non-ideal gaseous mixtures. The two processes involving H_2O self-relaxation,

$$H_2O(020) + H_2O \xrightarrow{k_a} H_2O(010) + H_2O \tag{A9}$$

and

$$H_2O(010) + H_2O \xrightarrow{k_b} H_2O + H_2O, \tag{A10}$$

were investigated experimentally. It was found that the rate of the relaxation from $2\nu_2$ -ν_2 was greater than that from ν_2 - 0 and potentially twice as fast. The following limits were assigned,

$$2k_a \geq k_b > k_a \tag{A11}$$

The channel

$$H_2O(020) + H_2O \rightarrow H_2O(010) + H_2O(010) \tag{A12}$$

was found to be insignificant in comparison. In Ref. A8, the relaxation of H_2O by rare gases was not studied in as much detail as the self-relaxation case.

c) V-R,T Relaxation of ν_2 Combination Levels ($\nu_1+\nu_2$, $\nu_2+\nu_3$)

For the SHARC reactions involving relaxation of one quantum of ν_2 from a combination level, the rate used for relaxation of the ν_2 level (k_1) can be used. The energy transferred is comparable in these three cases (1574 - 1593 cm^{-1}), and, therefore, the increase in rate as a function of temperature should also be similar.

$$M + H_2O(110) - M + H_2O(100);$$
$$k_{5\ forward} = 1.13 \times 10^{-10} \exp(-52.5/T^{.333}) \tag{A13}$$

$$M + H_2O(100) - M + H_2O(110);$$
$$k_{5\ reverse} = 1.13 \times 10^{-10} \exp(-52.5/T^{.333} - 2272.2/T) \tag{A14}$$

$$M + H_2O(011) - M + H_2O(001);$$
$$k_{6\ forward} = 1.13 \times 10^{-10} \exp(-52.5/T^{.333}) \tag{A15}$$

$$M + H_2O(001) - M + H_2O(011);$$
$$k_{6\ reverse} = 1.13 \times 10^{-10} \exp(-52.5/T^{.333} - 2268.5/T) \tag{A16}$$

The energies of the $\nu_1+\nu_2$, ν_1, $\nu_2+\nu_3$, and ν_3 band centers are 5235.0 cm^{-1}, 3657.08 cm^{-1}, 5331.279 cm^{-1}, and 3755.92 cm^{1}, respectively. The band center frequencies were used to obtain the energy level discrepancies for the reverse processes.

REFERENCES

A1. R.L. Taylor, Can. J. Chem., 52, 1436 (1974) [Review]

A2. R.G. Monk, J. Acoust. Soc. Amer. 46, 580 (1969). [295 K]

A3. H. E. Bass, R. G. Keeton and D. Williams, J. Acoust. Soc. Am., 60, 74 (1976). [400, 500, 600K]

A4. R.G. Keeton and H.E. Bass, J. Acoust. Soc. Am., 60, 78 (1976). 500 K]

A5. H.E. Bass and F. D. Shields, J. Acoust. Soc. Am., 56, 856 (1974). [400, 500, 600K]

A6. R. T. Kung and R.E. Center, J. Chem. Phys. 62, 2187 (1975). [1800-4100K]

A7. R. L. Rothman et al., *HITRAN 1991 Line List,* Phillips Laboratory/OPS (1991) and ibid., J. Quant. Spectrosc. Rad. Transfer, to be published.

A8. P. F. Zittel and D.E. Masturzo, J. Chem. Phys. 90, 977 (1989).

A9. F. E. Hovis and C.B. Moore, J. Chem. Phys., 72, 2397, (1980).

A10. P. F. Zittel and D.E. Masturzo, private communication based on J. Chem. Phys. 90, 977 (1989).

APPENDIX B

V-V RELAXATION OF H_2O BY O_2

a) Relaxation of the $H_2O(010)$ Level

The $O_2(1)$ level is only 38 cm^{-1} lower in energy than the $H_2O(010)$ level. This coincidence facilitates rapid resonant V-V energy transfer from $H_2O(010)$ to O_2. That is,

$$H_2O\,(010) + O_2(0) \overset{k_1}{=} H_2O(000) + O_2(1) \qquad \text{(B1)}$$

This process competes with the relaxation of H_2O (010) via the V-(R),T channels described in Appendix A. There have been no experiments to date designed to specifically separate the V-V and V-R,T contributions from the total relaxation rate of the $2\nu_2$ H_2O level by O_2. This would be a difficult task even using laser-induced fluorescence data since both amplitude subtraction as well as decay time separation is involved. Alternatively, if the assumption that $H_2O(010)$ relaxation by N_2 via a purely V-R,T mechanism is approximately equal to the V-R,T component of the relaxation by O_2, a reasonable approximation to the latter rate could be made. The V-R,T contribution could then be subtracted from the overall O_2 rate, leaving the V-V rate. This assumption is valid because there are no resonant V-V channels available with N_2.

For many kinetic applications, the rate determining step is the most important process. Since relaxation via a V-V energy transfer is often much faster than relaxation through a V-T channel, the faster rate is usually neglected. However, in modeling systems with high vibrational temperatures, such as H_2O in the thermosphere, the V-V fundamental relaxation rate of $H_2O(010)$ is used to infer rates for four other reversible relaxation processes from higher vibrational levels of H_2O by O_2. Each process involves the transfer of one quantum of ν_2 energy. Overall, the five processes involved could significantly affect the radiance from the H_2O bands. For this reason, it would be preferable to characterize the V-V and V-T rate constants explicitly.

In Taylor's 1974 review (Ref. B1), a temperature-independent rate of 1.0×10^{-12} cm^3 $molecule^{-1}$ s^{-1} was assumed for the forward rate of the reversible process, B1. This rate constant was based on a limited amount of theoretical information (Ref. B2).

Using the Tuesday-Boudart hypothesis (Ref. B3) for the five reversible energy transfer processes possible in a heated mixture of H_2O and O_2, Bass and Shields (Ref. 3, 1974), and later Bass, Keeton and Williams (Ref. 4, 1976) found rate constants for $k_{1\ reverse}$ at 400, 500 and 600 K. These were not direct measurements, but rather the results of an iterative procedure using experimental rates for three of the five processes in the mixture. The experimental values were from acoustic measurements. The data from each of the Bass references is plotted

in Fig. B1. The figure also contains a room-temperature theoretical prediction by Jones et al. (Ref. B5). Since several of the reported rates were for $k_{1\ reverse}$, they were converted to the corresponding forward rate constants using the $-E_1/T$ term (where $E_1 = 55.2$) before being plotted.

There is no temperature dependence evident over the very limited temperature range covered by the data in Fig. B1. The errors associated with the data vary from conservative estimates of 50% to an order of magnitude; therefore, the data did not warrant a full Landau-Teller fitting procedure. All of the data lie above or equal to the temperature-independent rate constant proposed by Taylor (Ref. B1) and used in previous versions of SHARC. Taylor's estimated constant is really a lower limit over the ~ 200 - 400 K range. The average of 9 data points, including one for Taylor's estimate, yields a rate constant of $k_{1\ forward} = 2.8 \pm .4 \times 10^{-12}$ cm^3 molecule^{-1} s^{-1}. As the temperature increases, the reverse process, relaxation of $O_2(1)$ by H_2O, will become slightly more significant. The energy discrepancy for the reverse process is 38.3 cm^{-1} so $k_{1\ reverse} = 2.9 \times 10^{-12} \exp(-55.8/T)$. However, apart from this shift in the population distribution between the $H_2O(010)$ and $O_2(1)$ states, a relatively small temperature dependence is expected for the rates of such resonant energy transfer processes.

b) V-V Relaxation from Higher Vibrational Levels

In previous versions of SHARC, the same lower limit to the rate of H_2O (010) V-V relaxation by O_2 was used for all the V-V relaxation processes of upper vibrational levels containing a ν_2 mode.

Applying the harmonic oscillator approximation to the rate of energy transfer from H_2O to O_2 by the V-V mechanism, we can multiply the rate for the H_2O (ν_2 - 0) process by factors of two and three for the ($2\nu_2$ - ν_2) and ($3\nu_2$ - $2\nu_2$) transitions, respectively. In units of cm^3 molecules^{-1} s^{-1}, the assigned rates are as follows:

$$H_2O(020) + O_2(0) = H_2O(010) + O_2(1);$$
$$k_{2\ forward} = 5.8 \times 10^{-12}$$
$$k_{2\ reverse} = 5.8 \times 10^{-12} \exp(-1.3/T) \qquad \text{(B2)}$$

$$H_2O(030) + O_2(0) = H_2O(020) + O_2(1);$$
$$k_{3\ forward} = 8.7 \times 10^{-12}$$
$$k_{3\ reverse} = 8.7 \times 10^{-12} \exp(58.8/T) \qquad \text{(B3)}$$

Two other near-resonant V-V energy transfer processes from higher combination levels of H_2O to the $O_2(1)$ level are possible:

$$H_2O(110) + O_2(0) = H_2O(100) + O_2(1);$$
$$k_{3\ forward} = 2.9 \times 10^{-12}$$
$$k_{3\ reverse} = 2.9 \times 10^{-12} \exp(-31.6/T) \quad \text{(B4)}$$

$$H_2O(011) + O_2(0) = H_2O(001) + O_2(1);$$
$$k_{3\ forward} = 2.8 \times 10^{-12}$$
$$k_{3\ reverse} = 2.8 \times 10^{-12} \exp(-27.8/T) \quad \text{(B5)}$$

The rate constants for Reactions B4 and B5 are approximately equal to k_1 since the ν_2 quantum number of the upper H_2O levels is one, and since only one quantum of energy from the ν_2 mode is transferred.

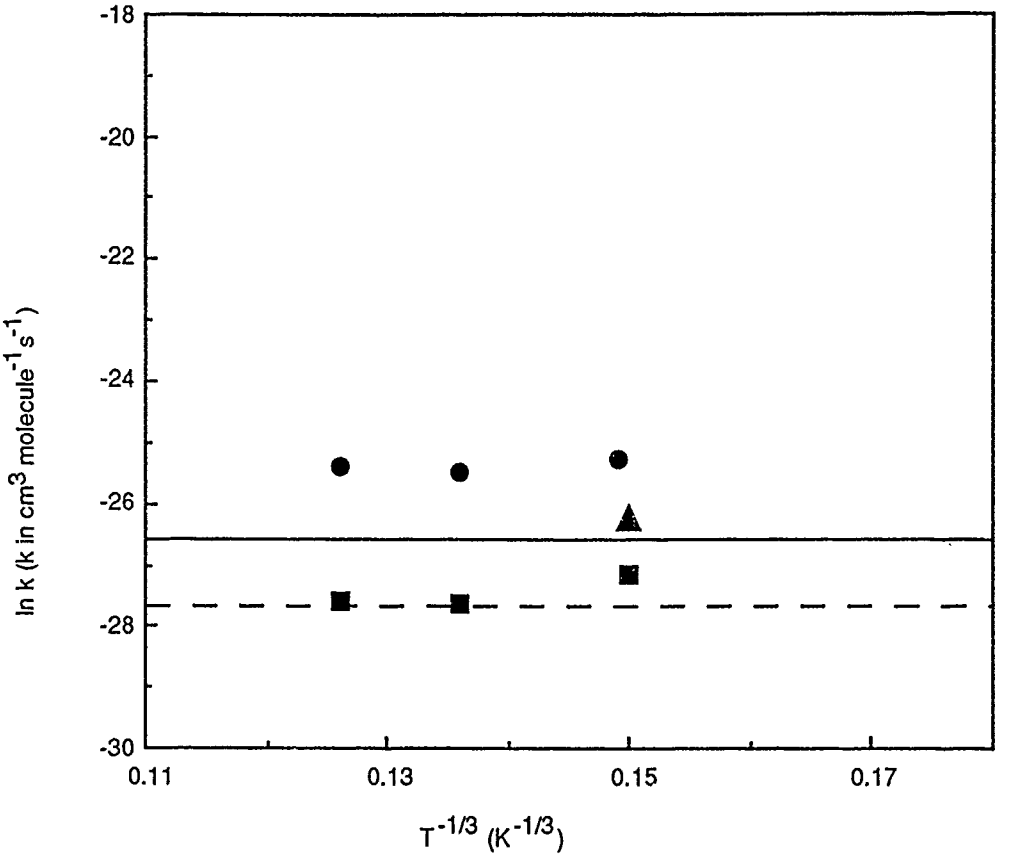

Figure B1. V-V relaxation of $H_2O(010)$ by O_2. Data from Bass, et. al. (Ref. B4), ● ; Jones et. al. (Ref. B5), ▲; Bass and Shields (Ref. B3), ■ . Average from this analysis ——. Constant from Taylor (Ref. B1), — – .

REFERENCES

B1. R. L. Taylor, Can. J. Chem., **52**, 1436 (1974).

B2. R. L. Taylor, S. Bitterman, Rev. Mod. Phys., **41**, 26 (1969).

B3. H. E. Bass and F. D. Shields, J. Acoust. Soc. Am., **56**, 856 (1974).

B4. H. E. Bass, R. G. Keeton and D. Williams, J. Acoust. Soc. Am., **60**, 74 (1976).

B5. D. G. Jones, J. D. Lambert and J.L. Stretton, Proc. Phys. Soc., **86**, 857 (1965).

APPENDIX C

V-R,T RELAXATION OF THE ν_1, ν_3 STRETCHING RESERVOIR AND COMBINATION LEVELS

a) $H_2O(100),(001)$ Relaxation by O_2, N_2

The energy difference between the band centers of the ν_1 and ν_3 stretching levels of H_2O is 99 cm^{-1}. Intramolecular energy transfer between these levels is facilitated by collision with a third body,

$$M + H_2O(001) \xrightarrow{k_1} H_2O(100) + M + 99\ cm^{-1} \qquad (C1)$$

Single collisions with a third body are probably enough to cause this intramolecular energy transfer in H_2O to occur at room temperature. The rapid equilibration between the (001) and (100) levels has been observed by Finzi et al. (Ref. C1). We estimate that the rate constant k_1 is gas kinetic at room temperature. Based on the collision cross-sections of H_2O and N_2, the temperature dependence is estimated to be

$$k_1 = 1.2 \times 10^{-11}\ T^{1/2} \qquad (C2)$$

The bidirectional interconversion, reaction C1, is rapid compared to that of energy transfer processes to lower vibrational levels. Furthermore, V-T energy transfer from either the ν_1 or ν_3 level to the $2\nu_2$ level (505 cm^{-1} or 604 cm^{-1} lower in energy, respectively) occurs at essentially the same rate.

One rate constant is assigned to both

$$H_2O(100) + M \xrightarrow{k_3} M + H_2O(020) \qquad (C3)$$

and

$$H_2O(001) + M \xrightarrow{k_4} M + H_2O(020) \qquad (C4)$$

Finzi et al. (Ref. B1) measured laser-induced fluorescence from the (ν_1, ν_3) reservoir to obtain a room temperature relaxation rate constant to the $H_2O(020)$ level. The experimentally measured quantity is actually a weighted average of k_3 and k_4. Their values for $k_{3\ forward}$ were 4.6 $\pm$ 1.2 x 10^{-13} cm^3 $molecule^{-1}$ s^{-1} for M = N_2 and 3.3 $\pm$ 1.2 x 10^{-13} cm^3 $molecule^{-1}$ s^{-1} for M = O_2. Efficiency coefficients of 1.0 and 0.7 are used to differentiate between the N_2 and O_2 rate constants in Table 1 and in SHARC. Unfortunately no information regarding the tempera-

ture dependence of these rate constants is yet available. Kung and Center (Ref. C2), who investigated other H_2O vibrational levels in their shock tube experiments, mention an overall rate for the relaxation at the stretch reservoir, but they included processes whereby $2\nu_2$ and ν_2 were relaxed to the ground state. They made the assumption that the latter step was rate determining; this was later disproven in the work of Finzi et al. Earlier rate constants suggested by Taylor (Ref. C3) or Sarjeant (Ref. C4) for the (ν_1, ν_3) reservoir relaxation were not based on experimental evidence specific to either Reaction C2 or C3.

The Finzi et al. room temperature rate constants of 4.6×10^{-13} and 3.3×10^{-13} cm^3 $molecule^{-1}$ s^{-1} for N_2 and O_2, respectively, were already incorporated into the kinetics scheme of earlier versions of SHARC, and, therefore, we have not recommended any changes.

b) Relaxation of $H_2O(110)$ and $H_2O(011)$ Combination Levels by O_2 and N_2

The following V-R,T energy transfer processes from combination levels are included in the H_2O kinetics scheme used in SHARC:

$$M + H_2O(110) \xrightarrow{k_5} M + H_2O(030) \qquad \text{(C5)}$$

and

$$M + H_2O(011) \xrightarrow{k_6} M + H_2O(030) \qquad \text{(C6)}$$

with M= O_2 or N_2. The energy difference between the $\nu_1 + \nu_2$ level and the $\nu_2 + \nu_3$ level is only 96 cm^{-1}. Therefore, rapid energy exchange will occur between the two levels, and they can be treated as a reservoir. Furthermore, processes 4 and 5 are analogous to processes 2 and 3 described in Part (a) of this appendix, that is, $k_2 \approx k_3 \approx k_5 \approx k_6$. A common room temperature rate constant is recommended. Again, the rate constants for N_2 and O_2 are differentiated by the efficiency factors of 1.0 and 0.7.

c) V-T Relaxation of the ν_1 and ν_2 Levels by Atomic Oxygen

The rate constant for processes C3 and C4 with $O(^3P)$ as the collision partner was measured by Zittel et al. (Ref. C5) at 315 K and 520 K using laser-induced fluorescence. The experimental values were $3(\pm 2) \times 10^{-12}$ cm^3 $molecule^{-1}$ s^{-1} and $5(\pm 3) \times 10^{-12}$ cm^3 $molecule^{-1}$ s^{-1}, respectively. There is insufficient data to establish a temperature trend so an average rate constant of 4×10^{-12} cm^3 $molecule^{-1}$ s^{-1} is recommended. In Table 1, the rate constant is reported as a collision efficiency parameter to the rate constant for Reaction C1.

The 1976 Standard model atmosphere (Ref. C6) indicates that at altitudes where $O(^3P)$ becomes a significant atmospheric constituent, the number density of H_2O has decreased to the extent that collisional relaxation of vibrationally excited H_2O by atomic oxygen is not

competitive with similar mechanisms involving N_2 or O_2. This conclusion is based on combining typical number densities for H_2O and $O(^3P)$ with the average rate constant for processes C3 and C4.

REFERENCES

C1. J. Finzi et al., J. Chem. Phys., **67** 4053 (1977).

C2. R. T. Kung and R. E. Center, J. Chem. Phys., **62**, 2187 (1975).

C3. R. L. Taylor, Can. J. Chem., **52,** 1381 (1974).

C4. W. J. Sarjeant et al. Appl. Opt., **11**, 735 (1972).

C5. P. F. Zittel and D. E. Masturzo, J. Chem. Phys., **90,** 978 (1989).

C6. *U. S. Standard Atmosphere, 1976,* NOAA, NASA and U.S. Air Force, Washington, D.C., pp. 212-227 (1976).

APPENDIX D

RATE CONSTANTS FOR SPONTANEOUS EMISSION PROCESSES FROM VIBRATIONALLY EXCITED H_2O

The 1991 HITRAN sum-of-lines band strengths (Ref. D1) given in Column 3 of Table D1 were used to calculate the Einstein A coefficients for spontaneous emission (in units of s^{-1}). The formula used for the calculation is that used in the SHARC 2.0 manual (Ref. D2) and in Ref. D3. That is,

$$A = \frac{8\pi c\nu^2 S_{ul}}{g_u} \frac{\exp[E_l/205.727]}{1-\exp[-\nu/205.727]} \quad . \tag{D1}$$

where ν is the transition frequency in cm^{-1} and E_l is the lower state energy in cm^{-1}. These and the other variables are described in references D2 and D3 as well as in the first report of this series (TR-0091(6078)-1). The units for S_{lu} are cm^{-1}/molecule/cm^2 or cm/molecule.

A comparison of our calculated A values and those used in earlier versions of SHARC indicated several discrepancies. Several of these differences were ≤ 10%. However, the ν_1 - 0, $3\nu_2$ - 0, $2\nu_2$ - ν_2, ν_1 - ν_2, and ν_3 - ν_2 Einstein A values were in much worse agreement. It appears that some of the spontaneous emission rate constants used in SHARC could have been derived from the dipole moments reported in the original references. The Einstein A coefficient calculated from the basic formula containing the transition moment R^{nm} and the frequency of the transition, ν, is (Ref. D4)

$$A = \frac{64\pi c\nu^3}{(4\pi\varepsilon_o)\, 3hc^3} |R^{nm}|^2 \tag{D2}$$

The latter calculation is complicated when there are Fermi interactions or Coriolis effects occurring. This is the case for the two sets of triad levels in H_2O. The interacting levels are ν_1, ν_3, and $2\nu_2$ in one set; and $3\nu_2$, $\nu_1+\nu_2$, and $\nu_2+\nu_3$ for the second set. Therefore, it is necessary to use a transformed dipole moment operator that includes a rotational operator, and a set of vibration-rotation wavefunctions for all three levels of the triad. The approximation that $|R^{nm}|^2 = |\mu|^2$ results in the A coefficients in Column 6 of Table D1. We did not pursue the detailed calculations involved for some of the other vibrational transitions via the dipole moment method.

Since Rothman's band strengths contain the best literature values to date for the rovibrational line strengths and, thus, the sum-of-line strengths, our recommendation is to standardize the Einstein A coefficients in the code by calculating them from Eqn. D1.

Table D1. Einstein A Coefficients for H_2O Vibrational Levels

BAND	Band Center Frequency (cm^{-1})	HITRAN Sum of Lines[D1] $cm^{-1}/(molecule\ cm^{-2})$	Einstein A from Sum of Lines (s^{-1})	Dipole Moment μ (D)	Einstein A Calculated from μ (s^{-1})	SHARC 2.0 A (s^{-1})
ν_1	3657.08[D5]	4.96×10^{-19}	5.00	-0.1532[D7]	3.61	3.37
ν_2	1594.74[D6]	1.06×10^{-17}	20.33	0.1269[D6]	20.47	18.35
ν_3	3755.92[D5]	7.20×10^{-18}	76.58	0.0686[D7]	78.34	78.40
$2\nu_2$	3151.63[D5]	7.57×10^{-20}	0.567	0.00581[D7]	---	0.454
$3\nu_2$	4666.8[D9]	3.96×10^{-22}	0.0065	0.209×10^{-4}[D8]	---	0.003
$\nu_1+\nu_2$	5235.0[D9]	3.72×10^{-20}	0.768	-0.002578[D8]	0.300	0.349
$\nu_2+\nu_3$	5331.279[D9]	8.04×10^{-19}	17.23	-0.019563[D8]	18.25	17.22
$2\nu_2 - \nu_2$	1556.89	9.71×10^{-21} (lit. 8.15×10^{-21})[D11]	41.29 34.65	0.1794[D11]	---	33.74
$\nu_1 - \nu_2$	2062.34	1.82×10^{-22}	1.36	0.447×10^{-2}[D11]	---	0.612
$\nu_3 - \nu_2$	2161.18	2.63×10^{-22}	2.15	0.0267[D11]	---	3.70
$3\nu_2 - \nu_2$	3072.06	7.30×10^{-23}	1.21	---	---	1.11
$(\nu_1+\nu_2) - \nu_2$	3640.26	1.95×10^{-22}	4.53	---	---	4.17
$(\nu_2+\nu_3) - \nu_2$	3736.54	2.92×10^{-21}	71.49	---	---	65.98
$3\nu_2 - 2\nu_2$	1515.17	5.14×10^{-24}	40.06	---	---	36.87

Superscripts [e.g., (D8)] refer to References D1 through D11.

REFERENCES

D1. L. S. Rothman et al., *HITRAN 1991 Line List* , Phillips Laboratory/OPS (1991) and ibid., J. Quant. Spectrosc. Rad. Transfer, to be published.

D2. R. D. Sharma et al., *Description of SHARC 2 The Strategic High-Altitude Atmospheric Radiance Code.*, PL-TR-91-2071, Phillips Laboratory, Hanscom Air Force Base, MA (1991), pp. 8.

D3. R. D. Sharma in *Modelling of the Atmosphere*, SPIE Volume 928 (1988), p. 187.

D4. J. M. Hollas, *High Resolution Spectroscopy*, Butterworths: Boston (1982), p. 46.

D5. R. A. Toth, J. Quant. Spectrosc. Radiat. Transfer **13**, 1127 (1973).

D6. C. Camy-Peyret and J. M. Flaud, Mol. Phys. **32**, 523 (1976).

D7. J. M. Flaud and C. Camy-Peyret, J. Mol. Spectrosc. **55**, 278 (1975).

D8. C. Camy-Peyret et al., ibid. **67**, 117 (1977).

D9. C. Camy-Peyret and J. M. Flaud, ibid. **59**, 327 (1976).

D10. J. M. Flaud and C. Camy-Peyret, ibid. **51**, 142 (1974).

D11. J. M. Flaud et al., Mol. Phys. **34**, 413 (1977).